

## Scaling of the anomalous Hall effect in SrRuO<sub>3</sub>

Noam Haham,<sup>1</sup> Yishai Shperber,<sup>1</sup> Moty Schultz,<sup>1</sup> Netanel Naftalis,<sup>1</sup> Efrat Shimshoni,<sup>1</sup> James W. Reiner,<sup>2</sup> and Lior Klein<sup>1</sup>  
<sup>1</sup>*Department of Physics, Nano-magnetism Research Center, Institute of Nanotechnology and Advanced Materials, Bar-Ilan University, Ramat-Gan 52900, Israel*

<sup>2</sup>*Hitachi Global Storage Technologies, 3403 Yerba Buena Rd, San Jose, CA 95315 USA*

(Received 27 October 2011; revised manuscript received 6 November 2011; published 28 November 2011)

We measure the anomalous Hall effect (AHE) resistivity  $\rho_{xy}$  in thin films of the itinerant ferromagnet SrRuO<sub>3</sub>. At low temperatures, the AHE coefficient  $R_s$  varies with  $\rho_{xx}^2$ , and at higher temperatures,  $R_s$  reaches a peak and then changes sign just below  $T_c$ . We find that for all films studied,  $R_s$  scales with resistivity in the entire ferromagnetic phase. We attribute the observed behavior to the contribution of the extrinsic side-jumps mechanism and the intrinsic Karplus-Luttinger (Berry phase) mechanism, including the effect of finite scattering rates.

DOI: [10.1103/PhysRevB.84.174439](https://doi.org/10.1103/PhysRevB.84.174439)

PACS number(s): 75.47.-m, 72.25.Ba, 75.50.Cc, 72.15.Gd

### I. INTRODUCTION

Being one of the most intriguing manifestations of a transport phenomenon that is sensitive to spin and topology, the anomalous Hall effect (AHE)<sup>1</sup> is the focus of considerable theoretical and experimental efforts. The interest in spin-sensitive phenomena is linked to the emerging field of spintronics,<sup>2</sup> which offers an alternative to conventional charge-based electronics. The interest in the effects of the topological features of bands on transport properties is linked to the role that these effects play in systems such as topological insulators and quantum Hall systems.<sup>3</sup>

The AHE is described phenomenologically as transverse resistivity  $\rho_{xy}^{\text{AHE}}$  or transverse conductivity  $\sigma_{xy}^{\text{AHE}}$  linked to the intrinsic magnetization  $\vec{M}$  of a conductor. Various models have been proposed: (a) The extrinsic model relates the AHE to antisymmetric scattering processes and it provides that

$$\rho_{xy}^{\text{AHE}} = R_s \mu_0 M_{\perp}, \quad (1)$$

where  $R_s = a\rho_{xx} + b\rho_{xx}^2$ , and  $M_{\perp}$  is the component of magnetization perpendicular to the film. The linear term in the resistivity of  $R_s$  is attributed to skew scattering<sup>4</sup> and it is expected to dominate in the high-conductivity regime ( $\sigma_{xx} > 10^6 \Omega^{-1} \text{cm}^{-1}$ ). The quadratic term is attributed to side jumps<sup>5</sup> and it is expected to dominate in the good conductivity regime ( $\sigma_{xx} \sim 10^4\text{--}10^6 \Omega^{-1} \text{cm}^{-1}$ ). (b) The intrinsic model known also as the Karplus-Luttinger model (K-L)<sup>6</sup> or Berry phase model attributes the AHE to intrinsic topological properties of the band.<sup>7,8</sup> According to this model,  $\rho_{xy}^{\text{AHE}} = \rho_{xx}^2 \sigma_{xy}(\vec{M})$ , and it is expected to dominate in the same regime as the side-jump mechanism. In the poor-conductivity regime ( $\sigma_{xx} < 10^4 \Omega^{-1} \text{cm}^{-1}$ ), a universal behavior  $\sigma_{xy} \sim \sigma_{xx}^{1.6-1.8}$  has been observed experimentally;<sup>9</sup> however, a theoretical understanding is still lacking. Interestingly, a similar scaling is predicted for metals in the limit of strong scattering due to finite-lifetime disorder broadening,<sup>10</sup> and within a microscopic model accounting for fluctuations of local orbital energies.<sup>11</sup>

SrRuO<sub>3</sub> has played a pivotal role in the study of the AHE and numerous attempts have been made to elucidate its complicated behavior. Berry phase calculations, which assume a temperature-dependent exchange gap that closes at  $T_c$ , seemed to describe the data reasonably.<sup>8</sup> However, a test of this scenario that focused on the vanishing point of the AHE

found that it vanishes for a given film (whose resistivity and magnetization were varied by field) at a specific resistivity, and not at a specific magnetization as one may expect from a scenario which attributes the vanishing signal of the AHE to the Berry phase contribution at a particular exchange splitting.<sup>12</sup> Midinfrared measurements suggest the applicability of the Berry phase scenario at energies above 200 meV, while the dc limit is dominated by extrinsic scattering mechanisms.<sup>13</sup>

By using SrRuO<sub>3</sub> films with a wide range of thicknesses that vary considerably in the temperature-dependence of their resistivity, we provide a compelling piece of evidence that resistivity, *irrespective of its sources or nature (elastic or inelastic)*, determines the AHE of SrRuO<sub>3</sub> in the entire ferromagnetic phase. This observation strongly suggests that changes in the Berry phase due to assumed temperature-dependent exchange splitting cannot explain the complicated temperature dependence of the AHE. We show that the side-jumps mechanism combined with the Karplus-Luttinger (Berry phase) mechanism that takes into account the scattering time may explain the observed behavior.

### II. SAMPLES AND EXPERIMENT

Our samples are epitaxial thin films of SrRuO<sub>3</sub> grown on slightly miscut ( $\sim 2^\circ$ ) substrates of SrTiO<sub>3</sub> by reactive electron-beam evaporation. The films are untwinned orthorhombic single crystals, with lattice parameters of  $a \cong 5.53$ ,  $b \cong 5.57$ , and  $c \cong 7.85 \text{ \AA}$ . The films were patterned to allow transverse and longitudinal resistivity measurements, which were performed with a Quantum Design PPMS-9. The films exhibit an exceptionally high resistivity ratio (up to 90), indicative of their high quality. The thinnest films ( $\leq 10 \text{ nm}$ ) exhibit a lower resistivity ratio ( $\geq 5$ ), which is still very high considering the enhanced surface scattering. Magnetic characterization of the films was performed using a Quantum Design SQUID magnetometer (MPMS).

Magnetic films may exhibit AHE if their magnetization has a component perpendicular to the film plane. As shape anisotropy favors in-plane magnetization, in many cases a perpendicular field should be applied in order to tilt the magnetization out of the plane. This may complicate the analysis since the applied field also induces the ordinary Hall effect (OHE).

SrRuO<sub>3</sub> films exhibit intrinsic uniaxial magnetocrystalline anisotropy with an easy axis, which varies with temperature between 45 degrees to the normal at  $T_c$  and 30 degrees at 2 K.<sup>14</sup> Moreover, the remanent magnetization is stable and spontaneous breakdown into magnetic domains occurs only a few degrees below  $T_c$ .<sup>15</sup> These features enable direct measurement of zero-field (remanent) antisymmetric transverse resistivity, which can be fully attributed to AHE,  $\rho_{xy}^{\text{AHE}}$ .

### III. EXPERIMENTAL RESULTS

Figure 1(a) shows the temperature dependence of  $\rho_{xy}^{\text{AHE}}$  of eight different samples. To extract  $R_s$  based on Eq. (1) [see Fig. 1(b)], we divide  $\rho_{xy}^{\text{AHE}}$  by  $M_{\perp}$  (shown in the inset). We note that for the thickness range of our samples,  $M_{\perp}$  is practically identical except for small deviations related to thickness-dependent  $T_c$ . This is expected, as thickness-induced changes in magnetic properties were reported for films with thickness lower than 6 nm.<sup>16</sup> We note that while  $R_s$  of the various samples has general common features, the variations

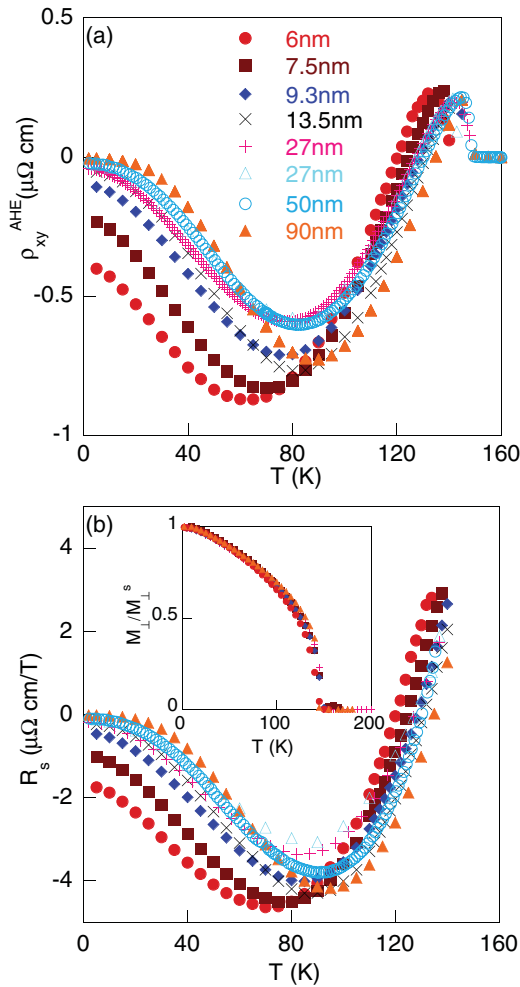


FIG. 1. (Color online) (a) Remanent AHE resistivity ( $\rho_{xy}^{\text{AHE}}$ ) of eight films vs temperature. (b) The AHE coefficient ( $R_s$ ) vs temperature derived from  $\rho_{xy}^{\text{AHE}}$  and  $M_{\perp}$  using Eq. (1). Inset: Scaling of the perpendicular magnetization ( $M_{\perp}$ ) normalized by its low temperature value as a function of temperature for five films with thickness between 6 and 90 nm.

are considerable. In particular, we note the differences in the values of  $R_s$  at 2 K, in the location of the negative peak and in the temperature at which  $R_s$  changes its sign. The large spread in  $R_s$  seems to correlate with changes in the resistivity of the films, strongly affected by film thickness [see Fig. 2(a)]. However, as seen in Fig. 2(b), the extracted  $R_s$  does not scale with  $\rho_{xx}$ . In particular, we note that the resistivity at which  $R_s$  changes its sign ( $\rho_0$ ) varies between 105  $\mu\Omega \text{ cm}$  for a 50-nm-thick sample to 202  $\mu\Omega \text{ cm}$  for a 6-nm-thick sample. Does this observation exclude the scenario that  $R_s$  is determined by  $\rho_{xx}$  in the entire ferromagnetic phase?—not necessarily.

Figure 3 shows that  $R_s^*$ , defined as  $R_s$  normalized by its maximum absolute value, does scale with  $\rho^*$ , defined as  $\rho_{xx}$  normalized by  $\rho_0$ . The scaling function has a quadratic dependence on  $\rho^*$  in the low resistivity regime (see inset) and it reaches its negative peak for all samples at  $\rho^* \cong 0.7$ .

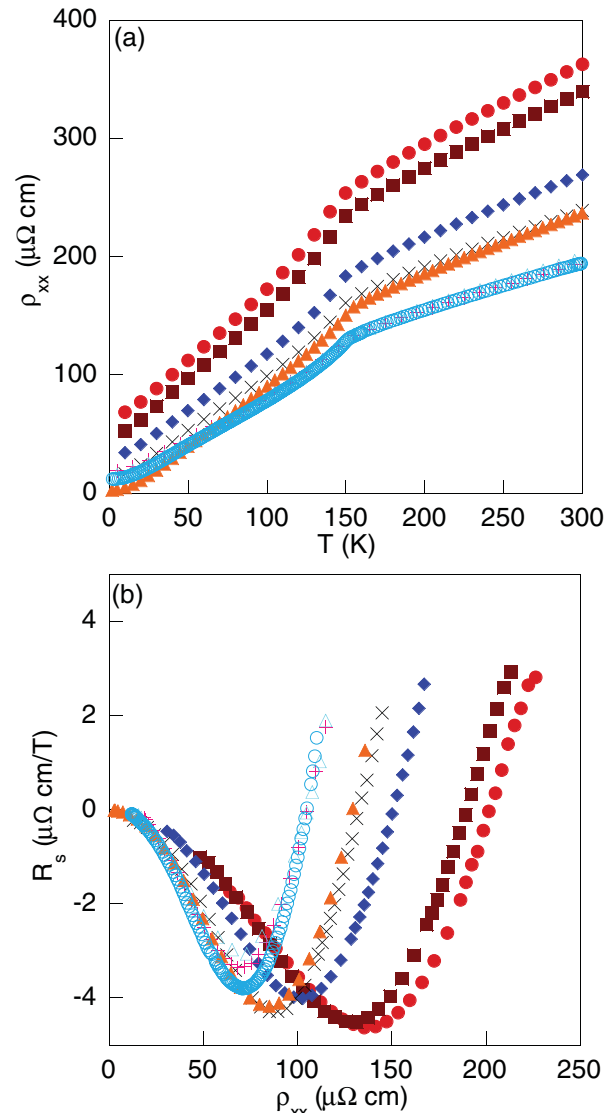


FIG. 2. (Color online) (a) Longitudinal resistivity ( $\rho_{xx}$ ) of the eight films presented in Fig. 1 vs temperature. (b)  $R_s$  from Fig. 1(b) vs resistivity ( $\rho_{xx}$ ).

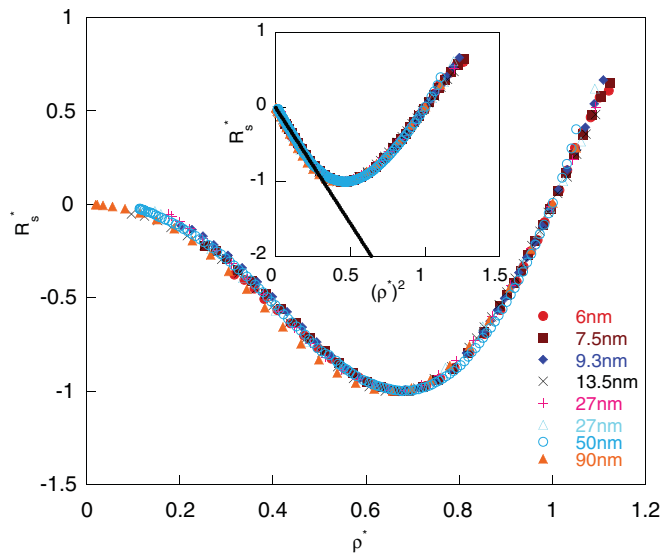


FIG. 3. (Color online)  $R_s$ , normalized by its absolute maximum value ( $R_s^*$ ) vs  $\rho_{xx}$  normalized by its value when  $R_s$  changes its sign ( $\rho^*$ ). Inset:  $R_s^*$  vs  $(\rho^*)^2$ .

A possible explanation for the striking scaling is that  $R_s$  is determined by  $\rho_{xx}$  and that it *does* vanish at the same intrinsic resistivity  $\rho_0^{\text{int}}$  for all samples, consistent with a previous report;<sup>12</sup> however, there is a multiplicative factor  $\gamma$  between the nominal resistivity and the intrinsic resistivity,  $\rho_{xx} = \gamma\rho_{xx}^{\text{int}}$ . A trivial source for  $\gamma$  is uncertainty in film thickness and in geometrical factors of the pattern. However, these sources alone cannot account for the observed variations on the order of fifty percent. Another potential source is dead layers<sup>16,17</sup> whose existence may considerably affect the calculated resistivity of ultrathin films. Assuming a dead layer of thickness  $\delta$ , we would expect  $\gamma = d/(d - \delta)$  and a linear dependence between  $d/\rho_0$  and  $d$ , as observed in the inset of Fig. 4. The linear fit is consistent with a dead-layer scenario with  $\delta \sim 3$  nm and  $\rho_0^{\text{int}} \sim 100 \mu\Omega \text{ cm}$ . The dead-layer scenario also implies that the resistivity of the various samples at high temperatures is not different [as suggested by Fig. 2(a)], but quite similar (Fig. 4). As the main difference between the films is in their thickness, the result supports the dead-layer scenario as it is expected that at high temperatures, where the mean free path is small and bulk scattering is dominant, the resistivity of our films would be similar.

The dead-layer scenario implies the need to normalize  $R_s$ ; however, its division by  $\gamma$  does not scale the data along the y axis. Therefore, the normalization of  $R_s$  with its maximum absolute value merely indicates that for all films, there is a single  $R_s(\rho_{xx})$  function up to a multiplicative factor.

We note that the scaling is obtained for films that vary considerably in their thickness and residual resistivity; namely, the same value of  $R_s$  is obtained for very different values of  $M_{\perp}$  and for very different contributions to  $\rho_{xx}$ . Thus, for instance,  $R_s$  attains its maximum value at  $T/T_c = 0.47$  for the 6-nm-thick film and at  $T/T_c = 0.63$  for the 90-nm-thick film. At this temperature, the magnetization is 84 percent (77 percent) of its low-temperature value for the thin (thick) film and the resistivity is 2 times (32 times) larger than its low-temperature

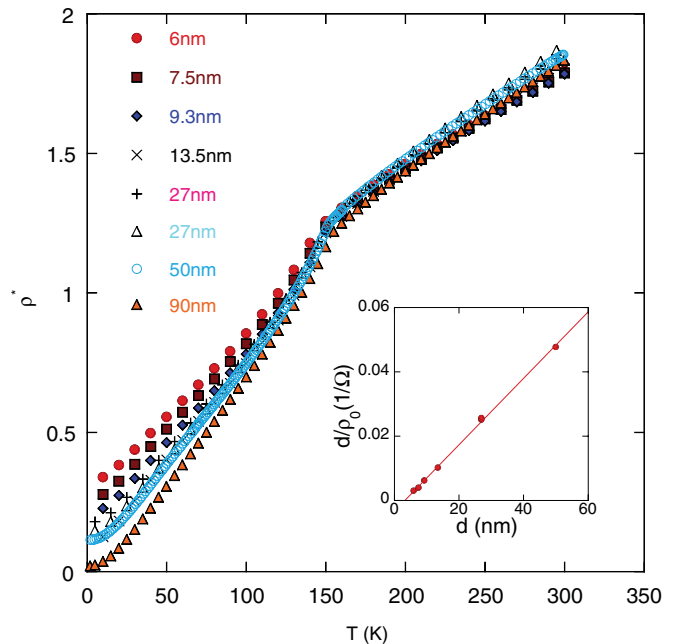


FIG. 4. (Color online) Normalized resistivity ( $\rho^*$ ) vs temperature. Inset: Film thickness ( $d$ ) divided by its resistivity when  $R_s$  changes its sign ( $\rho_0$ ) vs film thickness ( $d$ ).

value. Therefore, point defects, surface scattering, magnons, and phonons have very different weights in the two cases.

#### IV. THEORETICAL MODEL

The low temperature dependence of  $R_s$  on  $\rho_{xx}^2$  is consistent with the side-jumps mechanism<sup>5</sup> and with the Karplus-Luttinger (K-L) or Berry phase mechanism.<sup>6</sup> However, whereas side jumps can explain the scaling with  $\rho_{xx}$  due to its insensitivity to the scattering potential, it cannot explain the nonmonotonic temperature dependence, which includes a sign change at higher temperatures. On the other hand, attributing the nonmonotonic temperature dependence to the K-L mechanism, with a temperature-dependent exchange gap as suggested previously,<sup>8</sup> yields  $\rho_{xy}^{\text{AHE}} = \rho_{xx}^2 \sigma_{xy}(\mathbf{M})$  with a complicated dependence of  $\sigma_{xy}$  on  $\mathbf{M}$ , which is inconsistent with the scaling that assumes a linear dependence on  $M_{\perp}$ .

We now show that a combination of the side-jumps mechanism and the K-L mechanism, which considers the effect of the scattering rate and its temperature dependence (without assuming any change in the band structure), is a possible scenario. A consideration of the scattering rate ( $1/\tau$ ) effect on the transverse conductivity in the K-L mechanism is required in moderately good conductors, where  $\hbar/\tau$  is not negligible compared to the interband gap. The leading correction yields a decrease of  $\sigma_{xy}$  as the resistivity increases, and thus a possible nonmonotonic behavior of  $\rho_{xy}$ .

Accounting for a finite  $\tau$ , the K-L contribution to the AHE resistivity from Kubo's formula<sup>18</sup> becomes

$$\rho_{xy}^{K-L} = \rho_{xx}^2 e^2 \hbar / \Omega \times \sum_{n \neq m, k} \frac{\langle nk | v_y | mk \rangle \langle mk | v_x | nk \rangle [f(\epsilon_{n,k}) - f(\epsilon_{m,k})]}{[i(\epsilon_{m,k} - \epsilon_{n,k}) + \hbar/\tau](\epsilon_{n,k} - \epsilon_{m,k})}, \quad (2)$$

where  $\Omega$  is the crystal volume,  $k$  is the quasimomentum,  $n$  and  $m$  are band indices associated with the eigenvalues of the perfect crystal Hamiltonian,  $v_x$  and  $v_y$  are the velocity operators, and  $f(\varepsilon)$  is the Fermi-Dirac distribution. This contribution accounts only for the intrinsic part of the AHE, i.e., it ignores the corrections to the scattering processes due to spin-orbit interaction. We consider a model in which the main contribution to the sum in Eq. (2) is due to two bands denoted as 1, 2, where the Fermi level crosses the upper band while the lower band is fully occupied. We further assume that the dominant contribution arises from states with quasimomentum in a set denoted as  $\mathbb{K}$ , and that the energy gap for  $k \in \mathbb{K}$  between nonoccupied states in the upper level, and occupied states in the lower level, is approximately independent of quasimomentum and takes the characteristic value of  $\Delta$ . Under these assumptions, we obtain

$$\rho_{xy}^{K-L} = -\rho_{xx}^2 e^2 \hbar \left[ \frac{A}{(i\Delta + \hbar/\tau)\Delta} + \frac{A^*}{(-i\Delta + \hbar/\tau)\Delta} \right], \quad (3)$$

where  $A$  is defined as

$$A \equiv \int_{\mathbb{K}} \frac{d^3k}{2\pi^3} \langle 1k | v_y | 2k \rangle \langle 2k | v_x | 1k \rangle, \quad (4)$$

which can be associated with a Berry phase.<sup>1</sup> Since  $A$  is odd under time reversal and hence purely imaginary, we get

$$\rho_{xy}^{K-L} = -\rho_{xx}^2 e^2 \hbar \frac{2\text{Im}(A)}{\Delta^2 + (\hbar/\tau)^2}. \quad (5)$$

Considering spin-orbit interaction (SOI),  $A$  is expected to be proportional to  $M_{\perp}$ ;<sup>6</sup> namely,

$$\text{Im}(A) = aM_{\perp}, \quad (6)$$

where  $a$  is a constant. Previous reports indicate that the band structure in SrRuO<sub>3</sub> is temperature independent,<sup>19</sup> thus, ferromagnetism in SrRuO<sub>3</sub> should be described in the local band model.<sup>20</sup> Therefore, considering Eqs. (5) and (6) and averaging over the local magnetization yield

$$\rho_{xy}^{K-L} = -\rho_{xx}^2 e^2 \hbar \frac{2a}{\Delta^2 + (\hbar/\tau)^2} M_{\perp}, \quad (7)$$

where  $M_{\perp}$  is the averaged magnetization in the sample. Finally, we note that within the same level of approximation (i.e., leading order in the scattering potential), the side-jumps contribution is additive to the K-L term.<sup>21</sup> Thus, the AHE coefficient ( $R_s$ ) is given by a sum of the two contributions,

$$R_s = \rho_{xx}^2 \frac{B}{\Delta^2 + (\hbar/\tau)^2} + C\rho_{xx}^2. \quad (8)$$

The first term is the K-L term (with all the constants and the minus sign included in  $B$ ), and the second term is the side-jumps contribution. As  $B$ ,  $\Delta$ , and  $C$  are merely associated with the band structure, they are assumed to be constants. In the fit  $1/\tau$  is assumed to be proportional to  $\rho_{xx}$ , and the proportionality factor is estimated based on band calculations.<sup>22</sup> Thus, the right-hand side in Eq. (8) is a function of  $\rho_{xx}$  alone.

Figure 5 shows a fit of our data using Eq. (8), where the parameter  $C$  is limited to an interval which corresponds to a reasonable range of side jumps (0.1–10 Å)<sup>5</sup>. We obtain a good fit for side jumps in the range 1–10 Å, and  $\Delta$  in the range

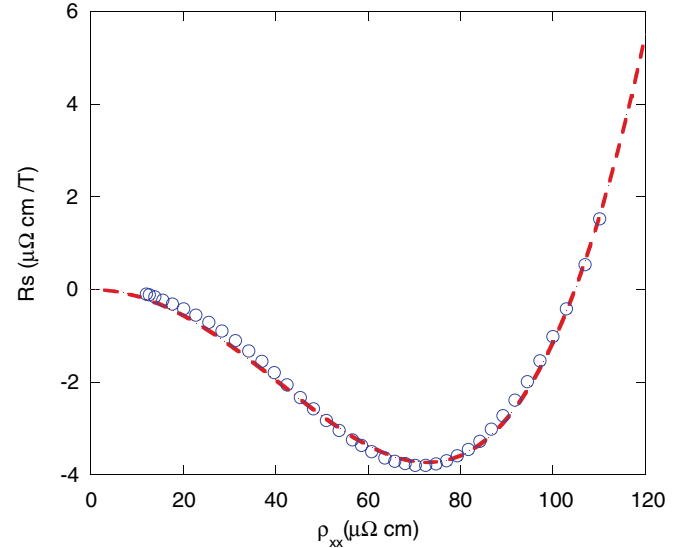


FIG. 5. (Color online) AHE coefficient  $R_s$  as a function of resistivity  $\rho_{xx}$  for a thick film (500 Å). The dashed line is a fit to Eq. (8).

0.07–0.2 eV. The value of  $\Delta$  is in good agreement with the characteristic energy at which  $\text{Im}(\sigma_{xy})$  has a peak, measured in the infrared regime for the low-temperature limit.<sup>13</sup> The fit presented in Fig. 5 is for a side jump of  $\sim 4$  Å and  $\Delta \sim 0.13$  eV. The fact that a similar temperature dependence of  $R_s$  is observed for other systems<sup>23</sup> suggests that this scenario is relevant to other materials as well.

## V. CONCLUSIONS

The scaling of  $\rho_{xy}^{\text{AHE}}$  data with  $\rho_{xx}$  in SrRuO<sub>3</sub> films implies that the AHE coefficient is determined by the total resistivity irrespective of the relative contributions of different scattering processes. To explain the scaling and the nonmonotonic behavior of the scaling function, we present a scenario that attributes the observed behavior to two contributions: (a) the side-jumps mechanism and (b) the K-L (Berry phase) mechanism, including the effect of finite scattering rates. In the limit of low resistivity, the two contributions have quadratic dependence on resistivity with coefficients of opposite signs, where that of the K-L term is larger. As resistivity increases, the K-L term decays due to the effect of finite scattering rates, which yields a sign change of  $\rho_{xy}^{\text{AHE}}$ .

## ACKNOWLEDGMENTS

We acknowledge useful discussions with J. S. Dodge, Y. Kats, and S. Simon. L.K. acknowledges support by the Israel Science Foundation founded by the Israel Academy of Sciences and Humanities (Grant No. 577/07). E.S. acknowledges support by the Israel Science Foundation (Grant No. 599/10), the US-Israel Binational Science Foundation (Grant No. 2008256), and the Aspen Center for Physics. J.W.R. grew the samples at Stanford University in the laboratory of M. R. Beasley.

- <sup>1</sup>N. Nagaosa, J. Sinova, S. Onoda, A. H. MacDonald, and N. P. Ong, *Rev. Mod. Phys.* **82**, 1539 (2010).
- <sup>2</sup>S. D. Bader and S. S. P. Parkin, *Annu. Rev. Condens. Matter Phys.* **1**, 71 (2010).
- <sup>3</sup>X. Qi and S. Zhang, *Phys. Today* **63**, 33 (2010).
- <sup>4</sup>J. Smit, *Physica* **21**, 877 (1955); **24**, 39 (1958).
- <sup>5</sup>L. Berger, *Phys. Rev. B* **2**, 4559 (1970); **5**, 1862 (1972).
- <sup>6</sup>R. Karplus and J. Luttinger, *Phys. Rev.* **95**, 1154 (1954).
- <sup>7</sup>T. Jungwirth, Q. Niu, and A. H. MacDonald, *Phys. Rev. Lett.* **88**, 207208 (2002); Y. Yao, L. Kleinman, A. H. MacDonald, J. Sinova, T. Jungwirth, D.-S. Wang, E. Wang, and Q. Niu, *ibid.* **92**, 037204 (2004).
- <sup>8</sup>Z. Fang, N. Nagaosa, K. S. Takahashi, A. Asamitsu, R. Mathieu, T. Ogasawara, H. Yamada, M. Kawasaki, Y. Tokura, and K. Terakura, *Science* **302**, 92 (2003); R. Mathieu, C. U. Jung, H. Yamada, A. Asamitsu, M. Kawasaki, and Y. Tokura, *Phys. Rev. B* **72**, 064436 (2005).
- <sup>9</sup>T. Fukumura, H. Toyosaki, K. Ueno, M. Nakano, T. Yamasaki, and M. Kawasaki, *Jpn. J. Appl. Phys.* **46**, L642 (2007); D. Venkateshvaran, W. Kaiser, A. Boger, M. Althammer, M. S. Ramachandra Rao, S. T. B. Goennenwein, M. Opel, and R. Gross, *Phys. Rev. B* **78**, 092405 (2008); W. R. Branford, K. A. Yates, E. Barkhударov, J. D. Moore, K. Morrison, F. Magnus, Y. Miyoshi, P. M. Sousa, O. Conde, A. J. Silvestre, and L. F. Cohen, *Phys. Rev. Lett.* **102**, 227201 (2009); T. Miyasato, N. Abe, T. Fujii, A. Asamitsu, S. Onoda, Y. Onose, N. Nagaosa, and Y. Tokura, *ibid.* **99**, 086602 (2007).
- <sup>10</sup>S. Onoda, N. Sugimoto, and N. Nagaosa, *Phys. Rev. B* **77**, 165103 (2008); *Phys. Rev. Lett.* **97**, 126602 (2006).
- <sup>11</sup>P. Streda, *Phys. Rev. B* **82**, 045115 (2010).
- <sup>12</sup>Y. Kats, I. Genish, L. Klein, J. W. Reiner, and M. R. Beasley, *Phys. Rev. B* **70**, 180407 (2004).
- <sup>13</sup>M.-H. Kim, G. Acbas, M.-H. Yang, M. Eginligil, P. Khalifah, I. Ohkubo, H. Christen, D. Mandrus, Z. Fang, and J. Cerne, *Phys. Rev. B* **81**, 235218 (2010).
- <sup>14</sup>L. Klein, J. S. Dodge, C. H. Ahn, J. W. Reiner, L. Mieville, T. H. Geballe, M. R. Beasley, and A. Kapitulnik, *J. Phys. Condens. Matter* **8**, 10111 (1996).
- <sup>15</sup>A. F. Marshall, L. Klein, J. S. Dodge, C. H. Ahn, J. W. Reiner, L. Mieville, L. Antagonazza, A. Kapitulnik, T. H. Geballe, and M. R. Beasley, *J. Appl. Phys.* **85**, 4131 (1999).
- <sup>16</sup>M. Schultz, S. Levy, J. W. Reiner, and L. Klein, *Phys. Rev. B* **79**, 125444 (2009).
- <sup>17</sup>R. P. Borges, W. Guichard, J. G. Lunney, J. M. D. Coey, and F. Ott, *J. Appl. Phys.* **89**, 3868 (2001); J. Z. Sun, D. W. Abraham, R. A. Rao, and C. B. Eom, *Appl. Phys. Lett.* **74**, 3017 (1999).
- <sup>18</sup>Y. Murayama, *Mesoscopic Systems: Fundamentals and Applications* (Wiley-VCH, Weinheim, Germany, 2001), pp. 213.
- <sup>19</sup>J. S. Dodge, E. Kulatov, L. Klein, C. H. Ahn, J. W. Reiner, L. Mieville, T. H. Geballe, M. R. Beasley, A. Kapitulnik, H. Ohta, Yu Uspenskii, and S. Halilov, *Phys. Rev. B* **60**, R6987 (1999).
- <sup>20</sup>V. Korenman, J. L. Murray, and R. E. Prange, *Phys. Rev. B* **16**, 4032 (1977); V. Korenman and R. E. Prange, *Phys. Rev. Lett.* **53**, 186 (1984).
- <sup>21</sup>H. Kontani, T. Tanaka, and K. Yamada, *Phys. Rev. B* **75**, 184416 (2007); A. Crepieux and P. Bruno, *ibid.* **64**, 014416 (2001).
- <sup>22</sup>G. Santi and T. Jarlborg, *J. Phys. Condens. Matter* **9**, 9563 (1997).
- <sup>23</sup>J. G. Checkelsky, M. Lee, E. Morosan, R. J. Cava, and N. P. Ong, *Phys. Rev. B* **77**, 014433 (2008).